Supplementary information to:

Extreme precipitation associated with atmospheric rivers over West Antarctic ice shelves: insights from kilometre-scale regional climate modelling

Ella Gilbert[1], Denis Pishniak[2], José Abraham Torres[3], Andrew Orr[1], Michelle Maclennan[4], Nander Wever[5], Kristiina Verro[6]

[1]British Antarctic Survey, Madingley Road, Cambridge, UK.
[2] National Antarctic Science Centre of Ukraine, Kyiv, Ukraine.
[3] Danish Meteorological Institute, Copenhagen, Denmark.
[4] University of Colorado Boulder, Boulder CO, USA.
[5] WSL Institute for Snow and Avalanche Research SLF, Davos, Switzerland.
[6] Institute for Marine and Atmospheric Research, Utrecht University, Utrecht, Netherlands.

Correspondence to: Ella Gilbert (ellgil82@bas.ac.uk)

Includes:
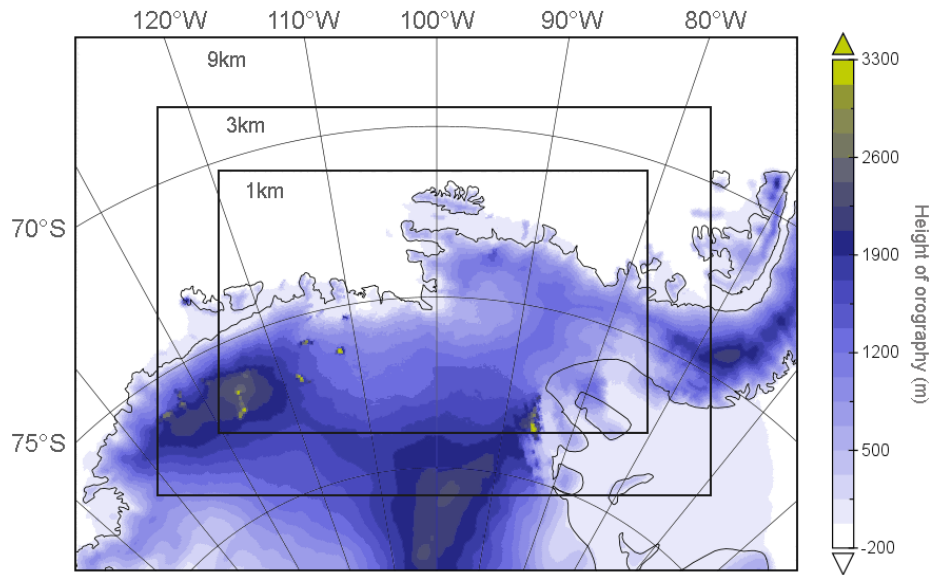
Figure S1. Model domains used in Polar-WRF. Colour contours show terrain height in the 9, 3 and 1 km resolution domains.

S1 Near-surface meteorology validation

S1.1 Time series over the Thwaites Glacier ice shelf

Figure S2 shows time series of near-surface meteorology during the summer and winter cases for 1.5 m temperature (a, e), 1.5 m relative humidity over water (b, f), surface pressure (c, g) and 10 m wind speed (d, h). Table S1 shows summary statistics for all models at both AWS stations, for the same near-surface meteorological variables. All RCMs compare well against observations, with ERA5 comparing most poorly, as discussed in the main text. None of the RCMs consistently out-perform the others, with HCLIM appearing to perform marginally better than Polar-WRF and the MetUM across all variables, seasons and stations.

As shown in Figure S2a, at the onset of the summer case, observed 1.5 m air temperatures on the TG ice shelf rise from values of below -5°C to near the freezing point of 0°C. Simultaneously, wind speeds (Figure S2d) and relative humidity (Figure S2b) increase, especially immediately following the passage of low-pressure systems shown in Figure S2c. This kind of signature in near-surface meteorological variables is characteristic of foehn winds (Gilbert et al., 2022) and is reproduced well by all three RCMs but not so well by ERA5. From then on, observed near-surface air temperatures during the summer case (Figure S2a) study hover around 0°C, reaching or exceeding 0°C for a total of 3.4 days during this case, suggesting that the surface may be warm enough to permit melting to occur. Indeed, mean MetUM-modelled surface temperatures at the Cavity and Channel stations are at the melt point for approximately 3.1 days and modelled surface temperatures reach the melt point somewhere on the TG ice shelf for 6.2 days of the 8-day case study.

All RCMs capture the main patterns of near-surface meteorology well in both cases, although PolarWRF and the MetUM exhibit considerable positive biases and high variability in relative humidity. Simulated relative humidity is reproduced especially badly by the MetUM and PolarWRF in the winter case (Figure S2f), reaching supersaturations of 120-140%, suggesting that the models are simulating cloud at the surface (i.e. fog) or surface precipitation much of the time. During summer MetUM- and PolarWRF-modelled relative humidity also briefly reaches super-saturation, but mainly relative humidity stays at or below 100% (Figure S2b).

As shown in Table S1, the RCMs consistently out-perform ERA5 for all four near-surface meteorological variables, with ERA5 exhibiting the largest biases and RMSEs and lowest correlation coefficients. This is especially true in summer. Of the models, there is no model that clearly performs best against all metrics for all variables. The MetUM represents temperature and surface pressure well in summer, and wind speed well in winter but represents relative humidity poorly in winter. Meanwhile, in winter PolarWRF represents wind speed and temperature fairly well and surface pressure poorly, while in summer PolarWRF does well with surface pressure and relative humidity. HCLIM performs reasonably well in both seasons, at both stations and for all variables, particularly for summer wind speed and relative humidity, and winter surface pressure.

Larger spatial variability, as indicated by the larger range of the shaded areas shown in Figure S2, is evident at the onset of the winter case (Figures S2e-h), which may suggest that localised processes are comparatively more important at this point of the case. This is also seen to a degree around the 6th February (summer case) when wind speeds rise (Figure S2d) and relative humidity falls (Figure S2b) by differing amounts across the ice shelf. This could be expected from a foehn warming effect that is most pronounced nearest the steepest

terrain but is not so large elsewhere on the ice shelf. In all RCMs, the range of values across the ice shelf is higher in winter than summer, suggesting that there may be considerable spatial variability in simulated humidity, which is at least partly related to the coincident variability in near-surface temperature. Periods with larger spatial variability in relative humidity also coincide with periods of higher winds, suggesting that moisture advection associated with the passage of ARs can have a strongly localised effect.

Table S1. Mean summary statistics during the winter and summer cases for near-surface meteorological variables, as simulated by all RCMs and ERA5, measured against AWS data from the Channel and Cavity stations. Statistics shown are mean bias, correlation coefficient (r^2), standard error (sterr) and root mean square error (RMSE) for near-surface air temperature (°C), relative humidity (%), surface air pressure (hPa) and 10 m wind speed (m s^{-1}). Model statistics are computed by taking the mean of the nine model grid points nearest to each AWS.

Season	Station	Model	Air temperature (°C)				Relative Humidity (%)				Surface pressure (hPa)				Wind speed (m s^{-1})			
			bias	r^2	sterr	RMSE	bias	r^2	sterr	RMSE	bias	r^2	sterr	RMSE	bias	r^2	sterr	RMSE
Summer	Cavity	MetUM	-0.20	0.98	0.018	0.49	5.19	0.71	0.10	7.54	0.76	0.99	0.012	1.29	0.79	0.74	0.06	2.35
		WRF	0.14	0.94	0.031	0.75	2.76	0.76	0.10	6.15	4.78	0.99	0.008	4.85	-0.51	0.69	0.05	2.29
		HCLIM	-0.06	0.96	0.016	0.76	4.43	0.72	0.06	5.75	0.96	0.99	0.011	1.35	0.05	0.75	0.05	2.08
		ERA5	-12.85	0.08	0.23	14.04	-12.55	0.06	0.15	15.60	19.63	-0.22	0.107	23.47	-1.30	-0.15	0.11	5.35
	Channel	MetUM	-0.08	0.97	0.019	0.47	5.29	0.69	0.10	7.83	1.33	0.99	0.012	1.71	1.13	0.69	0.06	2.65
		WRF	0.29	0.93	0.031	0.80	2.86	0.78	0.09	6.18	5.50	0.99	0.009	5.57	-0.16	0.65	0.06	2.42
		HCLIM	0.08	0.96	0.016	0.78	4.48	0.72	0.06	5.88	1.81	0.99	0.011	2.05	0.41	0.69	0.06	2.35
		ERA5	-15.21	0.48	0.176	15.78	-9.82	-0.08	0.10	12.67	-3.01	-0.15	0.123	13.93	3.83	-0.26	0.13	7.28
Winter	Cavity	MetUM	0.51	0.95	0.02	3.15	10.99	0.46	0.13	16.97	-0.93	0.99	0.010	1.62	0.54	0.62	0.04	4.09
		WRF	1.17	0.95	0.02	3.29	0.88	0.56	0.10	9.75	2.41	0.99	0.012	2.84	0.54	0.42	0.05	4.89
		HCLIM	0.42	0.92	0.03	3.76	-2.51	0.74	0.08	8.08	-0.26	0.99	0.009	1.20	-0.26	0.57	0.04	4.26
		ERA5	3.35	0.96	0.01	5.18	-2.98	0.79	0.06	6.78	-1.10	0.99	0.009	1.57	0.37	0.55	0.04	4.32
	Channel	MetUM	0.76	0.93	0.03	3.56	9.86	0.44	0.14	16.64	-1.00	0.96	0.020	2.73	2.73	0.33	0.03	8.32
		WRF	1.85	0.94	0.02	3.80	-0.08	0.58	0.11	10.07	2.50	0.95	0.023	3.77	-0.23	0.19	0.03	8.79
		HCLIM	0.77	0.91	0.03	4.04	-3.38	0.77	0.08	8.37	-0.02	0.97	0.019	2.30	-1.35	0.30	0.03	8.50
		ERA5	0.75	0.51	0.03	8.33	-3.17	0.07	0.08	10.12	-23.45	0.19	0.09	26.70	2.73	-0.34	0.04	11.64
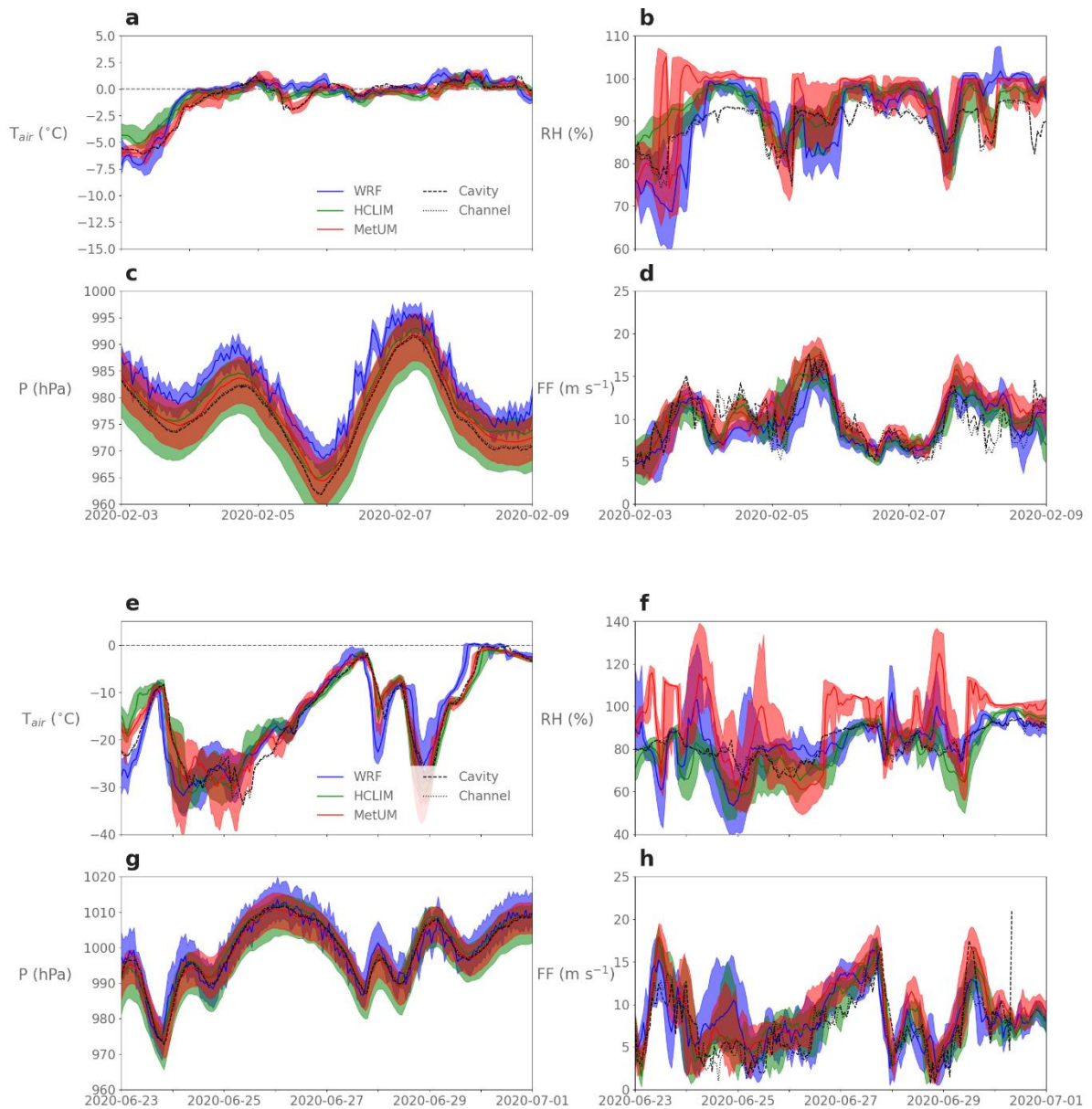
Figure S2. Time series of near-surface meteorology in observations and RCMs during the summer (top) and winter (bottom) cases: a, e) 1.5 m air temperature (°C), b, f) 1.5 m relative humidity (%), c, g) surface pressure (hPa) and d, h) 10 m wind speed (m s^{-1}). Model results are shown as averages across the entire TG ice shelf, with the ice shelf mean values indicated by the solid line. 1 km MetUM, Polar-WRF and HCLIM results are shown in red, blue and green, respectively, and the shaded regions show the 5th to 95th percentile range for each model. Panels a-d show the summer case and e-h show the winter case.

S2 Satellite-derived estimates of precipitation

S2.1 Satellite data description

Satellite-derived precipitation measurements are used for comparison against SNOWPACK, ERA5 and RCM simulations. We use the NASA Global Precipitation Measurement (GPM Integrated Multi-satellitE Retrievals for GPM (IMERG) product, which combines retrievals from a variety of satellites within the GPM constellation to produce a gridded precipitation dataset from passive, microwave and IR sensors at $0.1° \times 0.1°$ resolution (~12 km). Passive microwave data north of 60°S are masked over snowy/icy surfaces but are present at higher latitudes, including over part of our region of study. IMERG contains a 'probability of liquid precipitation' field, which can facilitate the diagnosis of precipitation phase. However, this variable cannot be used directly for partitioning precipitation amounts because it represents a probability that there is liquid precipitation falling somewhere within the gridbox, rather than the fraction of precipitation that is liquid. The field is globally complete and is generated exclusively from model/reanalysis data: MERRA2 for vertically integrated water vapour, Global Precipitation Climatology Centre monthly Monitoring Analysis for precipitation gauge analysis (global surface data) and ERA5 for precipitation retrievals. Further details are available in Huffman et al. (2023).

It is important to note that several of the sensors incorporated into the product can produce erroneous readings over cold land or sea ice (e.g. AMSR2, AMSR-E, SSMI, Eumetsat, MHS), which may introduce biases into the dataset (Huffman et al. (2023). Several studies report that the performance of IMERG is poor in cold regions, partly because passive microwave sensors are not used over snow/ice covered surfaces and ground-based sensors used in the algorithm are sparsely located, and partly because heavy solid precipitation and light liquid precipitation are both detected poorly (Pradhan et al., 2021; Eckert et al., 2022). IMERG is therefore an instructive dataset against which to compare the RCMs and observations, but it cannot be considered "truth" and is not necessarily a useful validation dataset. For this reason, we chose not to include it in the main text, but instead show it here for completeness.

S2.2 Evaluation of satellite-derived estimates of precipitation

Figure S3 shows snow and rainfall amounts over the TG and PIG ice shelves, as in Figure 4 in the main text but this time with GPM estimates also included in magenta. As shown in Figure S3 and as noted in the main text, satellite-derived estimates are extremely similar to those of ERA5 (reaching median values of 28 mm w.e and 19 mm w.e. over the TG and PIG ice shelves in summer), and considerably lower than the RCM estimates and SNOWPACK estimates. The similarity to ERA5 is expected because the precipitation product is partly generated using reanalysis data that has assimilated the same observations as ERA5.

Unfortunately it is difficult to compare the RCM simulations against the IMERG satellite data because the product does not separate liquid, solid or mixed phases of precipitation. While it does include a liquid precipitation probability, this diagnosis of liquid precipitation occurrence is based entirely on external datasets (reanalyses and the GPCC rain gauge network gridded product), which have poor resolution and/or coverage in the polar regions.

The maximum value of summertime GPM 'liquid probability' – which is the probability that precipitation is *exclusively* liquid or mixed phase – is around 3%, indicating that the satellite measurements assume that precipitation is entirely snow. As shown in the main text, all three RCMs simulate summer rainfall over the TG and PIG ice shelves, with ERA5 producing small amounts of rainfall in the regions with strongest foehn-driven warming. But as noted in the main text, only the highest resolution RCM nests feature significant rainfall, suggesting that cloud-resolving scale (< 10 km) and more sophisticated cloud microphysics are necessary to fully represent the kind of extreme conditions shown here, and that lower resolution products such as IMERG, the products it assimilates, and ERA5 may not fully capture these. This further emphasises the need for high-resolution RCMs for exploring extreme precipitation in this region.

However, the lower resolution of the IMERG product (~12 km) is not the only factor explaining why satellite estimates are lower than those from the RCMs, because the outermost nests of HCLIM and the MetUM – which are also at 12 km resolution – still have precipitation totals similar to those of the 1 km domains (Figure 6, main text). For example, the 12 km MetUM mean surface accumulated rain-to-snow ratio is approximately 0.17 over the Thwaites ice shelf and 0.40 over the PIG ice shelf, while the equivalent values are 0.37 and 0.53 for the 1 km domain. This suggests that the data ingested into the GPM IMERG product, as well as the assumptions made and the quality of the algorithms used in generating the precipitation estimates, may not accurately represent the dynamics and characteristics of extreme precipitation in this region. Hence, the high-resolution RCMs represent a more sophisticated method for evaluating the presence of liquid precipitation.
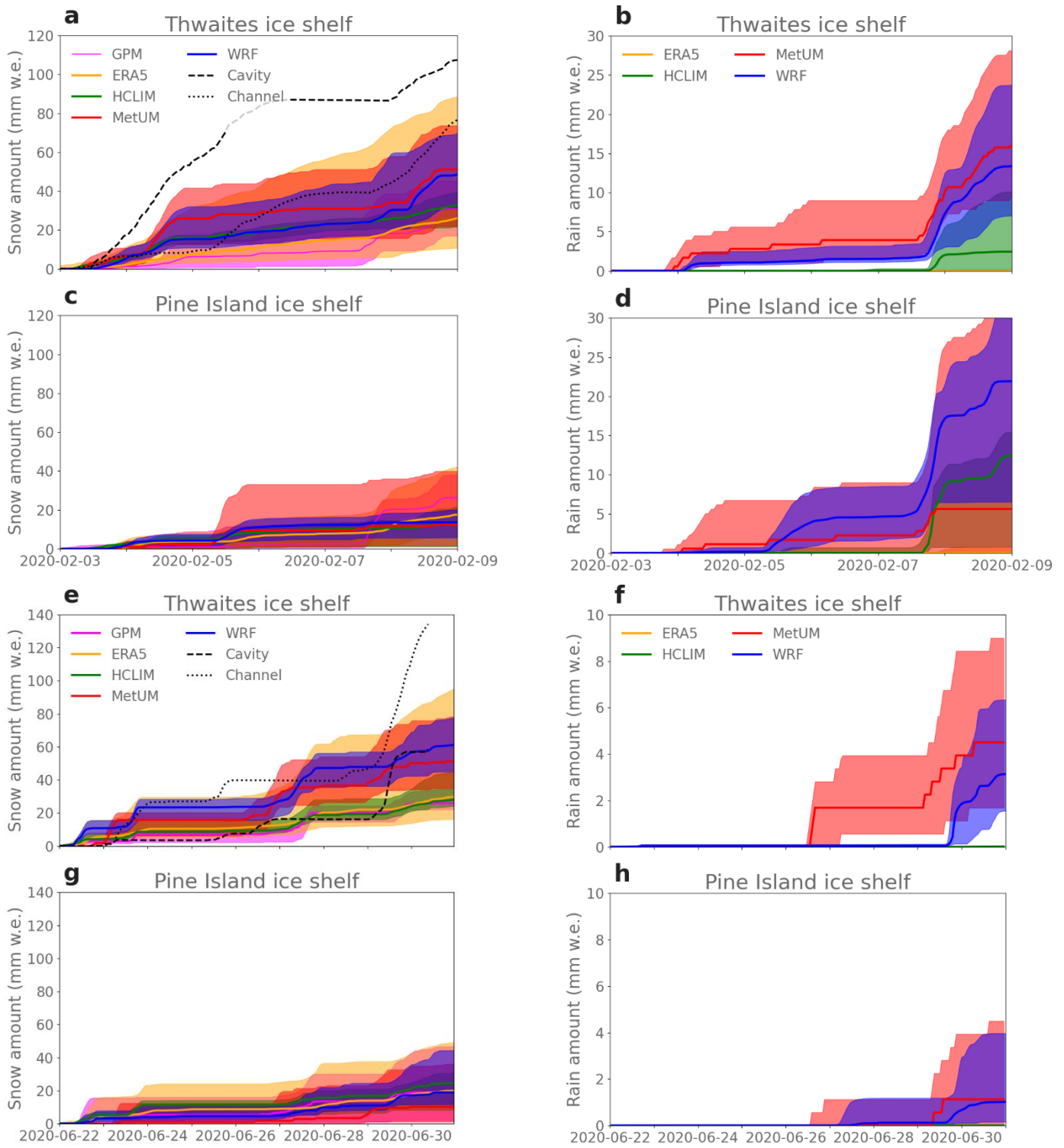
Figure S3. As in Figure 4, but including ice-shelf median precipitation amounts derived from the GPM IMERG product are also shown in magenta for comparison (note: these are *not* separated into snow or rain).
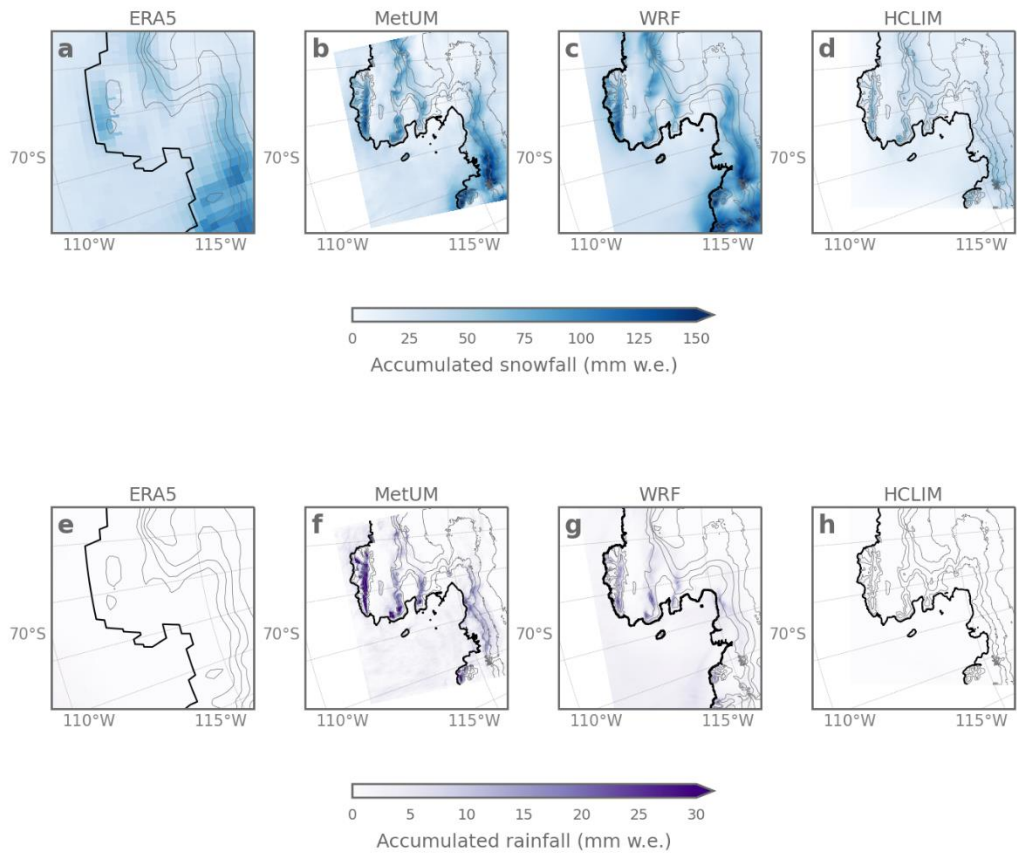
Figure S4. As in Figure 5 (main text) but for the winter case.

Summer
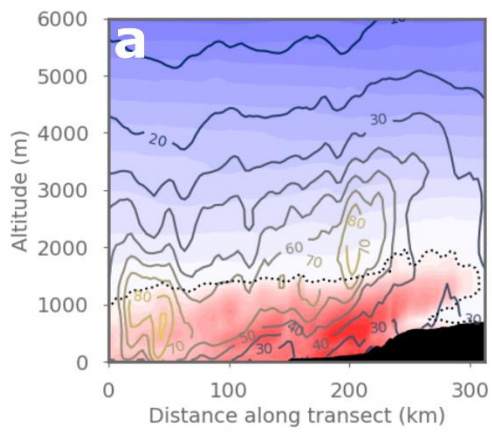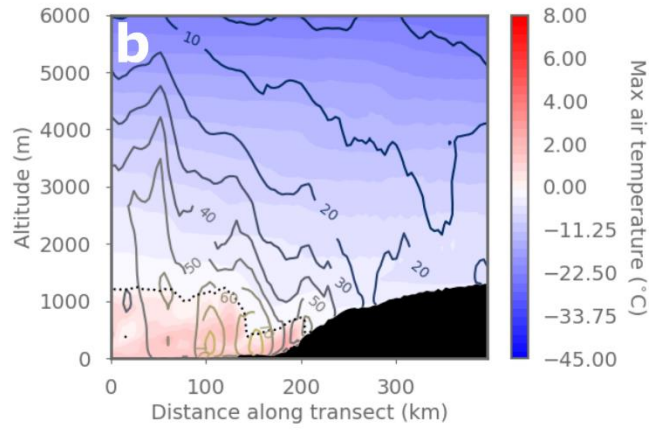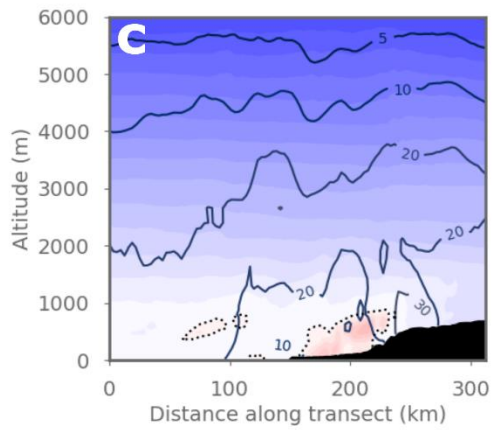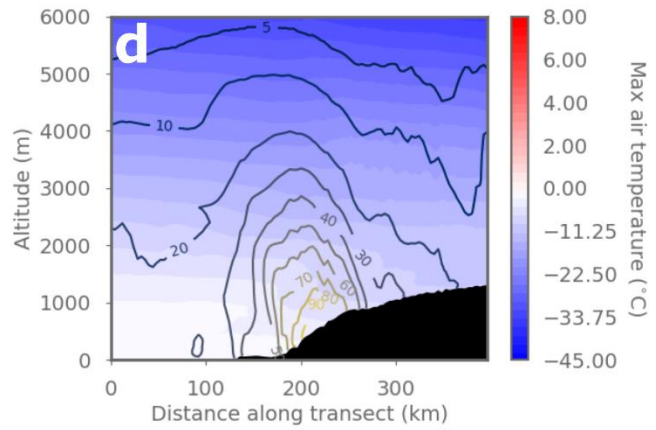
Figure S5. As in Figure 7, except for accumulated snowfall.

References

Eckert, E., Hudak, D., Mekis, É., Rodriguez, P., Zhao, B., Mariani, Z., ... & Walker, K. A. (2022). Validation of the Final Monthly Integrated Multisatellite Retrievals for GPM (IMERG) Version 05 and Version 06 with Ground-Based Precipitation Gauge Measurements across the Canadian Arctic. *Journal of Hydrometeorology*, *23*(5), 715-731. https://doi.org/10.1175/JHM-D-21-0040.1

Huffman, G.J., E.F. Stocker, D.T. Bolvin, E.J. Nelkin, Jackson Tan (2023), GPM IMERG Final Precipitation L3 Half Hourly 0.1 degree x 0.1 degree V07, Greenbelt, MD, Goddard Earth Sciences Data and Information Services Center (GES DISC), Accessed: *04 November 2023*, 10.5067/GPM/IMERG/3B-HH/07

Pradhan, R. K., Markonis, Y., Godoy, M. R. V., Villalba-Pradas, A., Andreadis, K. M., Nikolopoulos, E. I., ... & Hanel, M. (2022). Review of GPM IMERG performance: A global perspective. Remote Sensing of Environment, 268, 112754. https://doi.org/10.1016/j.rse.2021.112754